

Associated production of charged Higgs and top at LHC: the role of the complete electroweak supersymmetric contribution

M. Beccaria^{a,b}, G. Macorini^{a,b}, L. Panizzi^c, F.M. Renard^e and C. Verzegnassi^{c,d}

^a *Dipartimento di Fisica, Università del Salento, Italy*

^b *INFN, Sezione di Lecce, Italy*

^d *Dipartimento di Fisica Teorica, Università di Trieste, Italy*

^e *INFN, Sezione di Trieste, Italy*

^f *Laboratoire de Physique Théorique et Astroparticules,*

Université Montpellier II, France

Abstract

The process of charged Higgs production in association with a top quark at the LHC has been calculated at the complete NLO electroweak level both in a Two Higgs Doublets Model and in the Minimal Supersymmetric Standard Model, assuming a mSUGRA breaking scheme. We have numerically explored the size of the one-loop corrections in two typical supersymmetric scenarios, with particular attention to the $\tan\beta$ dependence, and we have found that they remain perturbatively small but possibly sizable, reaching a 20% limit for extreme values of $\tan\beta$, when the complete set of Feynman diagrams is taken into account.

PACS numbers:

I. INTRODUCTION

The processes of production of a charged Higgs boson will be extensively exploited to search for new physics beyond the standard model at the LHC. Most extensions of the Standard Model (SM), such as two-Higgs-doublet models (2HDM) or the Minimal Supersymmetric Standard Model (MSSM), enlarge the minimal SM Higgs sector predicting the existence of charged Higgs particle(s). Since the discovery of a charged Higgs boson would be a distinctive signature of new physics, an exhaustive comprehension of its production mechanism appears to be mandatory.

Depending on the charged Higgs boson mass, different production mechanisms are dominant: if $m_{H^+} < m_t - m_b$ the main source of charged Higgs is the $t\bar{t}$ production and the subsequent decay of the top $t \rightarrow H^+b$ [1], while for a heavier charged Higgs boson the dominant process is the associated production with heavy quarks [2]-[12]. Also the associated production with W gauge boson has been analysed [13]-[15], but this process is suppressed with respect to the other two mechanisms of production.

We will focus our analysis on the associated production with a top quark, which is also an important mechanism of top production and should be considered in the analysis of single top production at the LHC [16]. At the lowest perturbative order, it is well known that this process is particularly sensitive to the value of the parameter $\tan\beta$, *i.e.* the ratio of the neutral Higgs vacuum expectation values v_2/v_1 , which appears in the Yukawa coupling tbH . Being proportional to $m_b \tan\beta$, the coupling is enhanced for large values of $\tan\beta$ and this enhancement allows a direct check of the 2HDM structure of the model, not necessarily involving SUSY. Supersymmetric corrections, on the other hand, can be only investigated looking at the loop structure of the process.

Due to its relevance, the process of production of charged Higgs in association with a top quark has been extensively studied at higher orders and many important results have been obtained. The NLO corrections in QCD and SUSY QCD in the five-flavour scheme (*i.e.* including the bottom quark as a parton of the sea) have been computed in Refs. [7]-[11] and the same corrections in the four-flavour scheme, together with a comparison of the results in the two schemes have been computed in Ref. [12]. As a general feature, while QCD corrections are generally found to be large and positive and nearly independent of $\tan\beta$,

SUSY corrections appear to be sizable and negative for large $\tan\beta$. For what concerns the NLO electroweak (EW) contribution, the subset of Yukawa SUSY EW corrections has been computed in Refs. [4]-[6] in both the five- and four-flavour schemes: all of these papers assume that the Yukawa part of the correction is the leading one and they get some large one-loop contributions for “extreme” values of $\tan\beta$.

Given the possible relevance of the considered process, which might require a more accurate prediction, we have performed in this paper a complete NLO MSSM EW calculation. This includes all the EW diagrams that were neglected in the previous analyses and also the total QED radiation, that has never been computed for this process and whose effects might be *a priori* relevant, as we know from previous recent calculations of our group [17, 18].

The paper is organized as follows. Sect. II will be devoted to a description of the shape and of the basic properties of the parton level amplitudes for $bg \rightarrow tH^-$ at Born and at one-loop level. A rigorous treatment of QED radiation has been performed to obtain reliable values for the observables and will be described in Sect. II C. In Sect. III the numerical one-loop effects on the production rates and distributions for a couple of meaningful SUSY benchmark points will be shown, together with a discussion of the results.

II. KINEMATICS AND AMPLITUDES OF THE PROCESS $bg \rightarrow tH^-$

A. Kinematics

The kinematics of the process $bg \rightarrow tH^-$ is expressed in terms of the b quark momentum p_b , helicity λ_b , spinor $u(p_b, \lambda_b)$, the t quark momentum p_t , helicity λ_t , spinor $\bar{u}(p_t, \lambda_t)$, with:

$$p_b = (E_b; 0, 0, p) \quad p_t = (E_t; p' \sin \theta, 0, p' \cos \theta) , \quad (1)$$

the gluon momentum p_g , helicity λ_g , polarization vector e_g and the Higgs boson momentum p_H :

$$p_g = (p; 0, 0, -p) \quad e_g(\lambda_g) = \left(0; \frac{\lambda_g}{\sqrt{2}}, -\frac{i}{\sqrt{2}}, 0\right) \quad (2)$$

$$p_H = (E_H; -p' \sin \theta, 0, -p' \cos \theta) \quad (3)$$

We also use the s-channel and u-channel momenta:

$$q = p_g + p_b = p_H + p_t \quad s = q^2 \quad q' = p_t - p_g = p_b - p_H \quad u = q'^2 \quad (4)$$

The invariant amplitude of the process $b g \rightarrow t H^-$ will be decomposed on a set of 8 forms $J_{k\eta}$, where η represents the chirality R, L (sometimes denoted $\eta = +1, -1$). The 8 scalar functions $N_{k\eta}(s, t, u)$ will be computed in the next subsection from the various Born and one loop diagrams.

$$A = \sum_k J_{k\eta} N_{k\eta}(s, t, u) \quad (5)$$

$$J_{1\eta} = \not{p}_g \not{p}' P_\eta \quad J_{2\eta} = (e \cdot p_t) P_\eta \quad (6)$$

$$J_{3\eta} = \not{p}' P_\eta \quad J_{4\eta} = (e \cdot p_t) \not{p}_g P_\eta \quad (7)$$

with $P_\eta = P_{R,L} = (1 \pm \gamma^5)/2$.

The 8 helicity amplitudes $F_{\lambda_b, \lambda_g, \lambda_t}$ are obtained from Dirac decompositions of the 8 invariant forms.

Averaging over initial spins and colours and summing over final spins and colours with

$$\sum_{col} \langle \frac{\lambda^l}{2} \rangle \langle \frac{\lambda^l}{2} \rangle = 4 \quad (8)$$

one gets the elementary cross section:

$$\frac{d\sigma}{d \cos \theta} = \frac{\beta'}{768\pi s \beta} \sum_{spins} |F_{\lambda_b, \lambda_g, \lambda_t}|^2 \quad (9)$$

where $\beta = 2p/\sqrt{s}$, $\beta' = 2p'/\sqrt{s}$.

B. Born and one loop amplitudes

The Born terms result from the s-channel b exchange and the u-channel t exchange of Fig. 1:

$$A^{Born\ s} = -\left(\frac{g_s}{s - m_b^2}\right) \left(\frac{\lambda^l}{2}\right) \bar{u}(t) [c^L(b \rightarrow tH^-) P_L + c^R(b \rightarrow tH^-) P_R] (\not{q} + m_b) \not{p} u(b) \quad (10)$$

leads to the scalar function

$$N_{1\eta}^{Born\ s} = -g_s \left(\frac{\lambda^l}{2}\right) \frac{c^\eta(b \rightarrow tH^-)}{s - m_b^2} \quad (11)$$

and

$$A^{Born\ u} = -\left(\frac{g_s}{u - m_t^2}\right) \left(\frac{\lambda^l}{2}\right) \bar{u}(t) \not{p}' (\not{q}' + m_t) [c^L(b \rightarrow tH^-) P_L + c^R(b \rightarrow tH^-) P_R] u(b) \quad (12)$$

to

$$N_{1\eta}^{Born\ u} = -g_s \left(\frac{\lambda^l}{2}\right) \frac{c^\eta(b \rightarrow tH^-)}{u - m_t^2} \quad (13)$$

$$N_{2\eta}^{Born\ u} = -2g_s \left(\frac{\lambda^l}{2}\right) \frac{c^\eta(b \rightarrow tH^-)}{u - m_t^2} \quad (14)$$

with the btH^- couplings

$$c^L(b \rightarrow tH^-) = \frac{em_t \cot \beta}{\sqrt{2}s_W M_W} \quad c^R(b \rightarrow tH^-) = \frac{em_b \tan \beta}{\sqrt{2}s_W M_W} \quad (15)$$

The one loop EW terms can be classified as:

- counter terms for b, t, H^- lines and btH^- coupling constants. We follow the on-shell scheme in which all of the counter terms can be computed in terms of self-energy diagrams. For what concerns the H^- line and the btH^- coupling, we use the procedure given in [19] which takes into account the G^-, H^- mixing and expresses the counter term for $\tan \beta$ in terms of $W-H$ mixing self-energy. Other procedures, e.g. [20] or [21], would lead to a similar divergence cancellation but differ by minor finite contributions.
- self-energy corrections for internal b and t propagators;
- s-channel left triangles: $(Vqq), (Sqq), (\chi\tilde{q}\tilde{q})$ and right triangles: $(qSV), (Vq'q), (qVS), (Sf'f), (fSS')$;
- u-channel up triangles: $(ffV), (ffS), (SSf)$; and down triangles: $(VSq), (q'qV), (SVq), (f'fS), (S'Sf)$;
- direct boxes: $(qqq'V), (qqq'S), (\tilde{q}\tilde{q}\tilde{q}'\chi_j^-)$; crossed boxes: $(qqVS), (qqSV), (\tilde{q}\tilde{q}\chi_i\chi_j), (qqSS')$; twisted boxes: $(qqq'S), (qqq'V), (\tilde{q}\tilde{q}\tilde{q}'\chi_j)$.

All these contributions have been computed using the usual decomposition in terms of Passarino-Veltman functions and the complete amplitude has been implemented in the numerical code **PumaMC**.

We have checked the cancellation of the UV divergences among counter terms, self-energies and triangles. This cancellation occurs separately inside 8 sectors, i.e. s-left L or R, s-right L or R, u-up L or R, u-down L or R.

Another useful check can be done using the high energy behaviour of the amplitudes. High energy rules [22, 23] predict the logarithmic behaviour of these amplitudes at one loop level. They use splitting functions for external particles b, t, H and Renormalization Group effects on the parameters appearing in the Born terms.

By using the logarithmic expansions of the Passarino-Veltman functions [24] we have checked that the amplitudes obtained by summing the contributions of the above self-energy, triangle and box diagrams satisfy these rules.

At high energy we first observe the mass suppression of $N_3^{Born\ s+u}$ as well as the cancellation of $N_1^{Born\ s+u}$. One remains with only $N_2^{Born\ u}$ and the 2 helicity amplitudes $F_{-++,+--}$:

$$F_{-,+,+}^{Born} \rightarrow -\frac{eg_s m_t \cot \beta}{s_W M_W} \left(\frac{\lambda^l}{2}\right) \cos \frac{\theta}{2} \left(\frac{1 - \cos \theta}{1 + \cos \theta}\right) \quad (16)$$

$$F_{+,-,-}^{Born} \rightarrow -\frac{eg_s m_b \tan \beta}{s_W M_W} \left(\frac{\lambda^l}{2}\right) \cos \frac{\theta}{2} \left(\frac{1 - \cos \theta}{1 + \cos \theta}\right) \quad (17)$$

At one loop logarithmic level the aforementioned rules [22, 23] predict the corrections:

$$F_{-,+,+} = F_{-,+,+}^{Born} \{1 + \frac{1}{2}[c(b\bar{b}\ L) + c(t\bar{t}\ R)] + c_{-,+,+}^{ew}(H^-)\} \quad (18)$$

$$F_{+,-,-} = F_{+,-,-}^{Born} \{1 + \frac{1}{2}[c(b\bar{b}\ R) + c(t\bar{t}\ L)] + c_{+,-,-}^{ew}(H^-)\} \quad (19)$$

in which $c(b\bar{b}\ L)$, $c(t\bar{t}\ R)$ represent the b, t splitting functions and $c_{\mp, \pm, \pm}^{ew}(H^-)$ the total of the H^- splitting and of the parameter renormalization of the btH^- couplings through $\delta g/g - \delta M/M_W + \delta m_t/m_t - \delta \tan \beta / \tan \beta$ and $\delta g/g - \delta M_W/M_W + \delta m_b/m_b + \delta \tan \beta / \tan \beta$.

The result being:

$$F_{-,+,+} = F_{-,+,+}^{Born} \{1 + [\frac{\alpha}{4\pi}] \{ -[\frac{1}{3c_W^2}] \log^2 \frac{s}{m_Z^2} - [\frac{1}{9c_W^2}] \log^2 \frac{-t}{m_W^2} + \frac{1 - 4c_W^2}{12s_W^2 c_W^2} [\log^2 \frac{-u}{M_Z^2}] - \frac{1}{2s_W^2} [\log^2 \frac{-u}{M_W^2}] \} \} \quad (20)$$

$$F_{+,-,-} = F_{+,-,-}^{Born} \{1 + [\frac{\alpha}{4\pi}] \{ -[\frac{1 + 2c_W^2}{12s_W^2 c_W^2}] \log^2 \frac{s}{m_Z^2} - [\frac{1}{2s_W^2}] \log^2 \frac{s}{m_W^2} + \frac{1}{18c_W^2} [\log^2 \frac{-t}{M_W^2}] - \frac{1}{6s_W^2} [\log^2 \frac{-u}{M_W^2}] \} \} \quad (21)$$

with the absence of linear logarithmic terms as noticed in [25].

Taking our complete one loop computation and retaining only the logarithmic parts of the B,C,D Passarino-Veltman functions appearing in the various diagrams, we do recover the above expressions for the 2 leading amplitudes.

C. QED radiation

The computation of the real photon radiation contributions has been performed according to Ref. [26]. The matrix element has been calculated analytically with the help of `FeynArts` [27] and `FormCalc` [28]. Infrared (IR) singularities have been regularized within mass regularization, *i.e.* giving a small mass to the photon, and the phase space integration has been performed using the phase space slicing method.

Concerning the choice of the parton distribution functions (PDFs) and their factorization, we follow Ref. [26]. The PDFs used through this computation are the LO QCD parton distribution functions CTEQ6L [29]. The factorization of the bottom PDF has been performed in the \overline{MS} scheme at the scale $Q = (m_t + m_{H^-})$. If the DIS factorization scheme is used, the differences in the numerical value of the one-loop EW effects are of the order of 0.01% in all the considered mSUGRA benchmark points.

The phase space slicing method introduces a fictitious separator ΔE in the integration over the photon energy. As a check of our computations we have verified that, for sufficiently small ΔE values, the final cross section is independent on the choice of ΔE . Despite the strong sensitivity to ΔE of the soft and of the hard cross section, *c.f.* the upper panel of Fig. 2, the dependence of the total result on ΔE is far below the integration uncertainties (lower panel of Fig. 2).

III. ONE LOOP RESULTS

For the numerical evaluation of the one-loop corrections we have considered as SM inputs the values in Tab.I. The strong coupling constant has been evaluated at the renormalization scale $Q = m_t + m_{H^-}$ and its numerical value will be given below. Since we have performed our computations in the on-shell scheme, we have evaluated the pole mass of the bottom quark starting from the \overline{MS} mass at NLO in QCD, obtaining $m_b = 4.58$ GeV.

Coupling constants	$\alpha = 1/137.035999$ $\alpha_s(M_Z) = 0.118$
Gauge boson masses	$M_W = 80.424$ GeV $M_Z = 91.1876$ GeV
Quark Masses	$m_u = 47$ MeV $m_c = 1.55$ GeV $m_t = 170.9$ GeV $m_d = 47$ MeV $m_s = 0.15$ GeV $\overline{m_b}(\overline{m_b}) = 4.2$ GeV
Lepton Masses	$m_e = 0.51099906$ MeV $m_\mu = 105.6583$ MeV $m_\tau = 1.777$ GeV

Table I: Numerical values of SM inputs

As a first step, we have analysed the distributions of the invariant mass of the final states $d\sigma/dM_{inv}$ and the total cross section for a couple of representative SUSY benchmark points (assuming a mSUGRA supersymmetry breaking): LS2 [30] and SPS1a [31]. The characteristics of the benchmark points, together with the mass of the charged Higgs H^- and the value of $\alpha_s(Q)$, are shown in Tab. II. The two benchmarks are characterized by largely different input parameters at GUT scale, leading to different scenarios for low energy spectra: the LS2 point is an optimistic “light SUSY” scenario, while the SPS1a point is a standard and widely studied scenario for phenomenological analyses with higher masses. Moreover, the two points differ for the $\tan\beta$ values: LS2 features a very large $\tan\beta = 50$, while in SPS1a $\tan\beta = 10$. The complete spectra at low energy have been obtained running the parameters through the code `SUSPECT`[32]. The values of $\tan\beta$ at low energy have been translated from those obtained in the \overline{DR} scheme used by `SUSPECT` to the values in the on-shell scheme through the relation $\tan\beta(OS) = \tan\beta(\overline{DR}) - \delta \tan\beta(OS)|_{\text{finite}}$. The values we have obtained for LS2 and SPS1a are 60.5 and 10.4 respectively.

mSUGRA scenario	m_0	$m_{1/2}$	A_0	$\tan\beta$	sign μ	H^-	$\alpha_s(Q)$
LS2	300	150	-500	50	+	229.6	0.0965325
SPS1a	100	250	-100	10	+	412.1	0.0922963

Table II: input parameters for the mSUGRA benchmark points and mass of the charged Higgs H^- (all values with mass dimension are in GeV)

The resulting total cross sections and K-factors (where, as usual, $K = \sigma_{1-loop}/\sigma_{Born}$) are shown in Tab.III. Due to the very mild dependence of our calculations on the PDF factorization scheme, only the results obtained in the \overline{MS} scheme are shown. We have performed the analysis considering both the whole supersymmetric spectra (labelled “SUSY”

in the following discussion) and the “SUSY constrained” two-Higgs-doublet-model (2HDM) scenarios obtained from the original spectra considering only loops involving Higgs bosons and SM particles (*i.e.* without charginos, neutralinos and sfermions).

mSUGRA scenario	σ_{Born}	SUSY		2HDM	
		σ_{1-loop}	K-factor	σ_{1-loop}	K-factor
LS2	5.589	4.545	0.813	5.867	1.050
SPS1a	0.04207	0.04145	0.985	0.04170	0.991

Table III: Total cross sections (in pb) at Born and loop level and K-factors

It is possible to see that for both LS2 and SPS1a the corrections in the 2HDM subset are very small, of the order of few percent, while in the complete SUSY case the light LS2 spectrum features a bigger correction ($\sim 19\%$) than in the SPS1a case ($\sim 2\%$).

The differential distributions for the two benchmark points are shown in Fig. 3, where it is possible to see that, as a general behaviour, the one-loop corrections decrease from the low invariant mass region to high energies. In the SPS1a case (both SUSY and 2HDM) the one-loop corrections are positive near threshold, but suddenly drop and become negative at high energies: such compensating contributions are at the origin of the small one-loop correction to the total cross section. In LS2, on the other hand, SUSY and 2HDM behave in different ways: in the former case the one-loop corrections are always negative, the K-factor is ~ 0.97 near threshold and decreases at high energies with a behaviour analogous to the SPS1a case, thus explaining the large negative correction to the total cross section in this scenario; in the latter, the one-loop corrections are positive in a wider M_{inv} range, giving rise to the positive overall correction to the total cross-section.

As a second step in our analysis, given the relevance of $\tan\beta$ for the process under investigation, we have also analyzed the dependence of the K-factors on this parameter. Starting from the two previous LS2 and SPS1a spectra, we have considered $\tan\beta$ as a free parameter and varied it at low energy within a reasonable range. Chargino and neutralino masses and mixing matrices depend on the value of $\tan\beta$, and they have been varied accordingly. The results of the K-factors as a function of $\tan\beta$ for the LS2- and SPS1a-like spectra are shown in Fig. 4. It is possible to notice that the dependence of the K-factor is stronger in the LS2 case: in the complete SUSY scenario, it ranges from ~ 1 (low $\tan\beta$) to ~ 0.89 (large $\tan\beta$),

while the dependence in the 2HDM scenario shows opposite behaviour. One sees that the NLO effects remain perturbatively under control in the whole considered range, even for large values of $\tan\beta$, where corrections are usually expected to become large. Similar results have been found for the SPS1a-like spectra, where however, the dependence is milder than in the LS2-like case.

As a final remark, we can say that the dependence on the factorization scheme of our results is very mild, of the order of 0.01% in all the considered cases, and in Fig. 5 the differences between the two schemes are shown in more detail.

IV. CONCLUSIONS

In this paper we have calculated the complete EW NLO expression of the $bg \rightarrow tH^-$ process both in a 2HDM and in the MSSM, assuming a mSUGRA symmetry breaking scheme, to investigate the size of the corrections to tree-level observables and their $\tan\beta$ dependence. In our calculation we have included the full computation of QED radiation, which makes our analysis testable against future data. We have considered two benchmark points characterized by quite different values of $\tan\beta$ (10 and 50) and we have let the parameter vary into a reasonable range to investigate for dependences of the observables. We have found that the NLO corrections to the total cross sections can be sizable (negative and of the order of 20%) in the LS2 point, which is characterized by a light spectrum, and due to its cross sections (~ 5 pb) they might be hopefully observed at the LHC.

The dependence on $\tan\beta$ of the corrections is similar in the two benchmark points that we have analyzed, but more enhanced in LS2. On the other hand, the corrections exhibit a different behaviour in the two considered physical scenarios: in the 2HDM the corrections are generally mild, of the order of a few relative percent in the whole scanned range, and the effects raises for large $\tan\beta$; in the MSSM case, the one-loop corrections become negative and decreasing for large values of $\tan\beta$.

Given the outcome of our computations, we conclude that a complete calculation of EW MSSM NLO effects is worth and should be taken into account for a full, reliable and meaningful NLO analysis of this important process, which is probably the only one that can provide information on the charged Higgs couplings of the model.

Acknowledgements

We would like to thank Edoardo Mirabella for his contribution to the calculation of QED radiation and for valuable comments and suggestions.

Appendix A: COUNTER TERMS AND SELF-ENERGY CORRECTIONS TO BORN AMPLITUDES

In this appendix the expression of the counterterms are explicitly listed. They concern the counterterms for b , t , H^- lines as well as the propagator self-energy corrections for b and t exchanges.

s-channel counterterms

$$\begin{aligned}
 N_{1L}^{c.t. s} = & -\frac{g_s(\frac{\lambda^l}{2})}{s-m_b^2} \left\{ \frac{3}{2} \delta Z_L^b c^L(b \rightarrow tH^-) + \frac{1}{2} (\delta Z_R^t + \delta \psi_t) c^L(b \rightarrow tH^-) \right. \\
 & \left. + \delta c^L(b \rightarrow tH^-) + \frac{1}{2} \sum_j \delta Z_{j1}^* c^L(b \rightarrow tj) \right\}
 \end{aligned} \tag{A1}$$

$$\begin{aligned}
 N_{1R}^{c.t. s} = & -\frac{g_s(\frac{\lambda^l}{2})}{s-m_b^2} \left\{ \frac{3}{2} \delta Z_R^b c^R(b \rightarrow tH^-) + \frac{1}{2} (\delta Z_L^t + \delta \psi_t) c^R(b \rightarrow tH^-) \right. \\
 & \left. + \delta c^R(b \rightarrow tH^-) + \frac{1}{2} \sum_j \delta Z_{j1}^* c^R(b \rightarrow tj) \right\}
 \end{aligned} \tag{A2}$$

$$N_{3L}^{c.t. s} = \frac{m_b g_s(\frac{\lambda^l}{2})}{s-m_b^2} (\delta Z_R^b - \delta Z_L^b) c^R(b \rightarrow tH^-) \tag{A3}$$

$$N_{3R}^{c.t. s} = \frac{m_b g_s(\frac{\lambda^l}{2})}{s-m_b^2} (\delta Z_L^b - \delta Z_R^b) c^L(b \rightarrow tH^-) \tag{A4}$$

where, because of the $H^- - G^-$ mixing, we denote H^- by $j=1$ and G^- by $j=2$. And from b s.e. one gets ($\eta = +1, -1$ referring to R, L chiralities):

$$\begin{aligned}
 N_{1\eta}^{b \text{ s.e.}} = & g_s(\frac{\lambda^l}{2}) \frac{c^\eta(b \rightarrow tH^-)}{(s-m_b^2)^2} [s(\Sigma_\eta^b(s) + \delta Z_\eta^b) + m_b^2(\Sigma_{-\eta}^b(s) + \delta Z_{-\eta}^b) \\
 & + 2m_b^2(\Sigma_S^b(s) - \frac{1}{2}(\delta Z_\eta^b + \delta Z_{-\eta}^b) - \frac{\delta m_b}{m_b})]
 \end{aligned} \tag{A5}$$

$$\begin{aligned}
 N_{3\eta}^{b \text{ s.e.}} = & g_s(\frac{\lambda^l}{2}) \frac{c^{-\eta}(b \rightarrow tH^-) m_b}{(s-m_b^2)} [\Sigma_\eta^b(s) + \delta Z_\eta^b + \Sigma_S^b(s) \\
 & - \frac{1}{2}(\delta Z_\eta^b + \delta Z_{-\eta}^b) - \frac{\delta m_b}{m_b}]
 \end{aligned} \tag{A6}$$

u-channel counterterms

$$\begin{aligned}
N_{1L}^{ct\ u} &= -g_s \left(\frac{\lambda^l}{2}\right) \frac{1}{(u - m_t^2)} \left\{ \left(\frac{3}{2}\delta Z_R^t + \frac{1}{2}\delta\psi_t + \frac{1}{2}\delta Z_L^b\right) c^L(b \rightarrow tH^-) \right. \\
&\quad \left. + \delta c^L(b \rightarrow tH^-) + \frac{1}{2} \sum_j \delta Z_{j1}^* c^L(b \rightarrow tj) \right\} \tag{A7}
\end{aligned}$$

$$\begin{aligned}
N_{1R}^{ct\ u} &= -g_s \left(\frac{\lambda^l}{2}\right) \frac{1}{(u - m_t^2)} \left\{ \left(\frac{3}{2}\delta Z_L^t + \frac{1}{2}\delta\psi_t + \frac{1}{2}\delta Z_R^b\right) c^R(b \rightarrow tH^-) \right. \\
&\quad \left. + \delta c^R(b \rightarrow tH^-) + \frac{1}{2} \sum_j \delta Z_{j1}^* c^R(b \rightarrow tj) \right\} \tag{A8}
\end{aligned}$$

$$\begin{aligned}
N_{2L}^{ct\ u} &= -2g_s \left(\frac{\lambda^l}{2}\right) \frac{1}{(u - m_t^2)} \left\{ \left(\frac{3}{2}\delta Z_R^t + \frac{1}{2}\delta\psi_t + \frac{1}{2}\delta Z_L^b\right) c^L(b \rightarrow tH^-) \right. \\
&\quad \left. + \delta c^L(b \rightarrow tH^-) + \frac{1}{2} \sum_j \delta Z_{j1}^* c^L(b \rightarrow tj) \right\} \tag{A9}
\end{aligned}$$

$$\begin{aligned}
N_{2R}^{ct\ u} &= -2g_s \left(\frac{\lambda^l}{2}\right) \frac{1}{(u - m_t^2)} \left\{ \left(\frac{3}{2}\delta Z_L^t + \frac{1}{2}\delta\psi_t + \frac{1}{2}\delta Z_R^b\right) c^R(b \rightarrow tH^-) \right. \\
&\quad \left. + \delta c^R(b \rightarrow tH^-) + \frac{1}{2} \sum_j \delta Z_{j1}^* c^R(b \rightarrow tj) \right\} \tag{A10}
\end{aligned}$$

$$N_{3L}^{ct\ u} = g_s \left(\frac{\lambda^l}{2}\right) \frac{m_t c^L(b \rightarrow tH^-)}{(u - m_t^2)} \{\delta Z_R^t - \delta Z_L^t\} \tag{A11}$$

$$N_{3R}^{ct\ u} = g_s \left(\frac{\lambda^l}{2}\right) \frac{m_t c^R(b \rightarrow tH^-)}{(u - m_t^2)} \{\delta Z_L^t - \delta Z_R^t\} \tag{A12}$$

and from t s.e. one gets:

$$\begin{aligned}
N_{1\eta}^{t\ s.e.} &= g_s \left(\frac{\lambda^l}{2}\right) \frac{c_\eta(b \rightarrow tH^-)}{(u - m_t^2)^2} \left[u(\Sigma_{-\eta}^t(u) + \delta Z_{-\eta}^t) + m_t^2(\Sigma_\eta^t(u) + \delta Z_\eta^t) \right. \\
&\quad \left. + 2m_t^2(\Sigma_S^t(u) - \frac{1}{2}(\delta Z_\eta^t + \delta Z_{-\eta}^t) - \frac{\delta m_t}{m_t}) \right] \tag{A13}
\end{aligned}$$

$$N_{2\eta}^{t\ s.e.} = 2N_{1\eta}^{t\ s.e.} \tag{A14}$$

$$N_{3\eta}^{t\ s.e.} = g_s \left(\frac{\lambda^l}{2}\right) \frac{c_\eta(b \rightarrow tH^-) m_t}{(u - m_t^2)} \left[\Sigma_\eta^t(u) + \delta Z_\eta^t + \Sigma_S^t(u) - \frac{1}{2}(\delta Z_\eta^t + \delta Z_{-\eta}^t) - \frac{\delta m_t}{m_t} \right] \tag{A15}$$

The c.t. appearing in the above expressions are obtained in terms of self-energies as follows:

b and t quark

$$\delta Z_L^b = \delta Z_L^t \equiv \delta Z_L = -\Sigma_L^b(m_b^2) - m_b^2[\Sigma_L^{\prime b}(m_b^2) + \Sigma_R^{\prime b}(m_b^2) + 2\Sigma_S^{\prime b}(m_b^2)] \quad (\text{A16})$$

$$\delta Z_R^b = -\Sigma_R^b(m_b^2) - m_b^2[\Sigma_L^{\prime b}(m_b^2) + \Sigma_R^{\prime b}(m_b^2) + 2\Sigma_S^{\prime b}(m_b^2)] \quad (\text{A17})$$

$$\delta Z_R^t = \delta Z_L + \Sigma_L^t(m_t^2) - \Sigma_R^t(m_t^2) \quad (\text{A18})$$

$$\delta \Psi_t = -\{\Sigma_L^t(m_t^2) + \delta Z_L + m_t^2[\Sigma_L^{\prime t}(m_t^2) + \Sigma_R^{\prime t}(m_t^2) + 2\Sigma_S^{\prime t}(m_t^2)]\} \quad (\text{A19})$$

$$\delta m_b = \frac{m_b}{2} \text{Re}[\Sigma_L^b(m_b^2) + \Sigma_R^b(m_b^2) + 2\Sigma_S^b(m_b^2)] \quad (\text{A20})$$

$$\delta m_t = \frac{m_t}{2} \text{Re}[\Sigma_L^t(m_t^2) + \Sigma_R^t(m_t^2) + 2\Sigma_S^t(m_t^2)] \quad (\text{A21})$$

gauge boson

$$\delta Z_1^W - \delta Z_2^W = \frac{\Sigma^{\gamma Z}(0)}{s_W c_W M_Z^2} \quad (\text{A22})$$

$$\delta Z_2^W = -\Sigma^{\prime \gamma \gamma}(0) + 2\frac{c_W}{s_W M_Z^2} \Sigma^{\gamma Z}(0) + \frac{c_W^2}{s_W^2} \left[\frac{\delta M_Z^2}{M_Z^2} - \frac{\delta M_W^2}{M_W^2} \right] \quad (\text{A23})$$

$$\delta M_W^2 = \text{Re} \Sigma^{WW}(M_W^2) \quad \delta M_Z^2 = \text{Re} \Sigma^{ZZ}(M_Z^2) \quad (\text{A24})$$

Higgs boson

We need δZ_{j1}^* which means $\delta Z_{H^-H^-}^*$ and $Z_{G^-H^-}^*$. We use the on-shell procedure of Wan et al [19] in which

$$\delta Z_{H^-H^-} = -\Sigma'_{H^-}(p^2 = m_{H^-}^2) \quad (\text{A25})$$

and

$$\delta Z_{G^-H^-}^* = \delta Z_{G^+H^+} = -\frac{2\Sigma_{H^-W^-}^*(m_{H^-}^2)}{M_W} = \frac{2\Sigma_{H^+W^+}(m_{H^+}^2)}{M_W} \quad (\text{A26})$$

Couplings

The Yukawa btH^- coupling leads to the c.t. δc^L and δc^R , computed in terms of δg , $\delta m_{t,b}$, δM_W (given above) and $\delta \tan \beta$. For the latter, we have adopted the renormalization scheme of [19].

$$\frac{\delta c^L}{c^L} = \frac{\delta g}{g} + \frac{\delta m_t}{m_t} - \frac{\delta M_W}{M_W} - \frac{\delta \tan \beta}{\tan \beta} \quad (\text{A27})$$

$$\frac{\delta c^R}{c^R} = \frac{\delta g}{g} + \frac{\delta m_b}{m_b} - \frac{\delta M_W}{M_W} + \frac{\delta \tan \beta}{\tan \beta} \quad (\text{A28})$$

$$\frac{\delta g}{g} = \delta Z_1^W - \frac{3}{2} \delta Z_2^W \quad (\text{A29})$$

$$\frac{\delta \tan \beta}{\tan \beta} = \frac{\text{Re} \Sigma_{H+W+}(m_{H^+}^2)}{M_W \sin 2\beta} \quad (\text{A30})$$

-
- [1] Z. Kunszt and F. Zwirner, Nucl. Phys. B **385** (1992) 3 [arXiv:hep-ph/9203223].
- [2] V. D. Barger, R. J. N. Phillips and D. P. Roy, Phys. Lett. B **324** (1994) 236 [arXiv:hep-ph/9311372];
- [3] C. S. Huang and S. H. Zhu, Phys. Rev. D **60** (1999) 075012 [arXiv:hep-ph/9812201].
- [4] L. G. Jin, C. S. Li, R. J. Oakes and S. H. Zhu, Phys. Rev. D **62**, 053008 (2000) [arXiv:hep-ph/0003159].
- [5] A. Belyaev, D. Garcia, J. Guasch and J. Sola, Phys. Rev. D **65**, 031701 (2002) [arXiv:hep-ph/0105053].
- [6] A. Belyaev, D. Garcia, J. Guasch and J. Sola, JHEP **0206** (2002) 059 [arXiv:hep-ph/0203031].
- [7] S. h. Zhu, Phys. Rev. D **67**, 075006 (2003) [arXiv:hep-ph/0112109].
- [8] T. Plehn, *Prepared for 10th International Conference on Supersymmetry and Unification of Fundamental Interactions (SUSY02), Hamburg, Germany, 17-23 Jun 2002*
- [9] T. Plehn, Phys. Rev. D **67**, 014018 (2003) [arXiv:hep-ph/0206121].
- [10] G. p. Gao, G. r. Lu, Z. h. Xiong and J. M. Yang, Phys. Rev. D **66** (2002) 015007 [arXiv:hep-ph/0202016].
- [11] E. L. Berger, T. Han, J. Jiang and T. Plehn, Phys. Rev. D **71**, 115012 (2005) [arXiv:hep-ph/0312286].
- [12] S. Dittmaier, M. Kramer, M. Spira and M. Walser, arXiv:0906.2648 [hep-ph].
- [13] D. A. Dicus, J. L. Hewett, C. Kao and T. G. Rizzo, Phys. Rev. D **40** (1989) 787.
- [14] A. A. Barrientos Bendezu and B. A. Kniehl, Phys. Rev. D **59** (1999) 015009 [arXiv:hep-ph/9807480].
- [15] W. Hollik and S. h. Zhu, Phys. Rev. D **65** (2002) 075015 [arXiv:hep-ph/0109103].
- [16] W. Bernreuther, J. Phys. G **35** (2008) 083001 arXiv:0805.1333 [hep-ph].
- [17] M. Beccaria, C. M. Carloni Calame, G. Macorini, G. Montagna, F. Piccinini, F. M. Renard and C. Verzegnassi, Eur. Phys. J. C **53** (2008) 257, arXiv:0705.3101 [hep-ph].
- [18] M. Beccaria, C. M. Carloni Calame, G. Macorini, E. Mirabella, F. Piccinini, F. M. Renard and C. Verzegnassi, Phys. Rev. D **77** (2008) 113018, arXiv:0802.1994 [hep-ph].
- [19] L. H. Wan, W. G. Ma, R. Y. Zhang and Y. Jiang, Phys. Rev. D **64** (2001) 115004 [arXiv:hep-ph/0107089].

- [20] H. Eberl, M. Kincel, W. Majerotto and Y. Yamada, Phys. Rev. D **64** (2001) 115013 [arXiv:hep-ph/0104109].
- [21] A. Freitas and D. Stockinger, [arXiv:hep-ph/0210372].
- [22] M. Beccaria, F. M. Renard and C. Verzegnassi, [arXiv:hep-ph/0203254].
- [23] M. Beccaria, M. Melles, F. M. Renard, S. Trimarchi and C. Verzegnassi, Int. J. Mod. Phys. A **18** (2003) 5069 [arXiv:hep-ph/0304110].
- [24] M. Beccaria, G. J. Gounaris, J. Layssac and F. M. Renard, Int. J. Mod. Phys. A **23** (2008) 1839, arXiv:0711.1067 [hep-ph].
- [25] M. Beccaria, F. M. Renard and C. Verzegnassi, arXiv:0904.2646 [hep-ph].
- [26] M. Beccaria, G. Macorini, E. Mirabella, L. Panizzi, F. M. Renard and C. Verzegnassi, arXiv:0812.4375 [hep-ph].
- [27] J. Kublbeck, M. Bohm and A. Denner, Comput. Phys. Commun. **60**, 165 (1990).
T. Hahn, Comput. Phys. Commun. **140**, 418 (2001) [arXiv:hep-ph/0012260].
T. Hahn and C. Schappacher, Comput. Phys. Commun. **143**, 54 (2002) [arXiv:hep-ph/0105349].
- [28] T. Hahn and M. Perez-Victoria, Comput. Phys. Commun. **118**, 153 (1999) [arXiv:hep-ph/9807565].
T. Hahn and M. Rauch, Nucl. Phys. Proc. Suppl. **157**, 236 (2006) [arXiv:hep-ph/0601248].
- [29] J. Pumplin, D. R. Stump, J. Huston, H. L. Lai, P. M. Nadolsky and W. K. Tung, JHEP **0207**, 012 (2002) [arXiv:hep-ph/0201195].
- [30] M. Beccaria, G. Macorini, F. M. Renard and C. Verzegnassi, Phys. Rev. D **74**, 013008 (2006) [arXiv:hep-ph/0605108].
- [31] B. C. Allanach *et al.*, *The Snowmass points and slopes: Benchmarks for SUSY searches*, in *Proc. of the APS/DPF/DPB Summer Study on the Future of Particle Physics (Snowmass 2001)* ed. N. Graf, *In the Proceedings of APS / DPF / DPB Summer Study on the Future of Particle Physics (Snowmass 2001), Snowmass, Colorado, 30 Jun - 21 Jul 2001, pp P125* [arXiv:hep-ph/0202233].
- [32] A. Djouadi, J. L. Kneur and G. Moultaka, Comput. Phys. Commun. **176** (2007) 426 [arXiv:hep-ph/0211331].

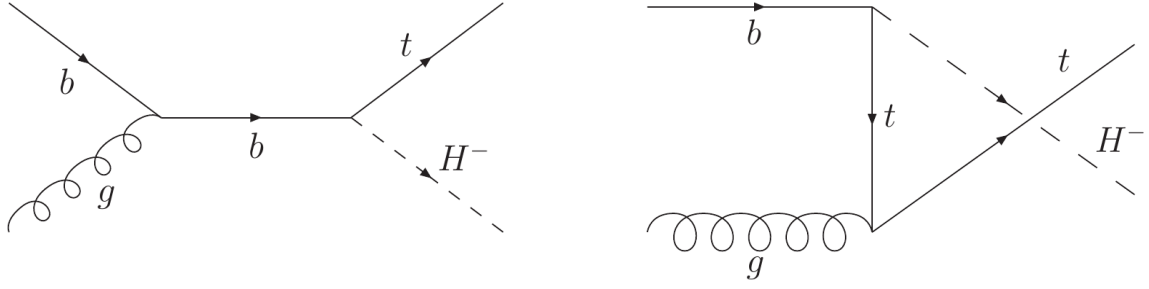


Figure 1: Born diagrams: s-channel bottom exchange and u-channel top exchange.

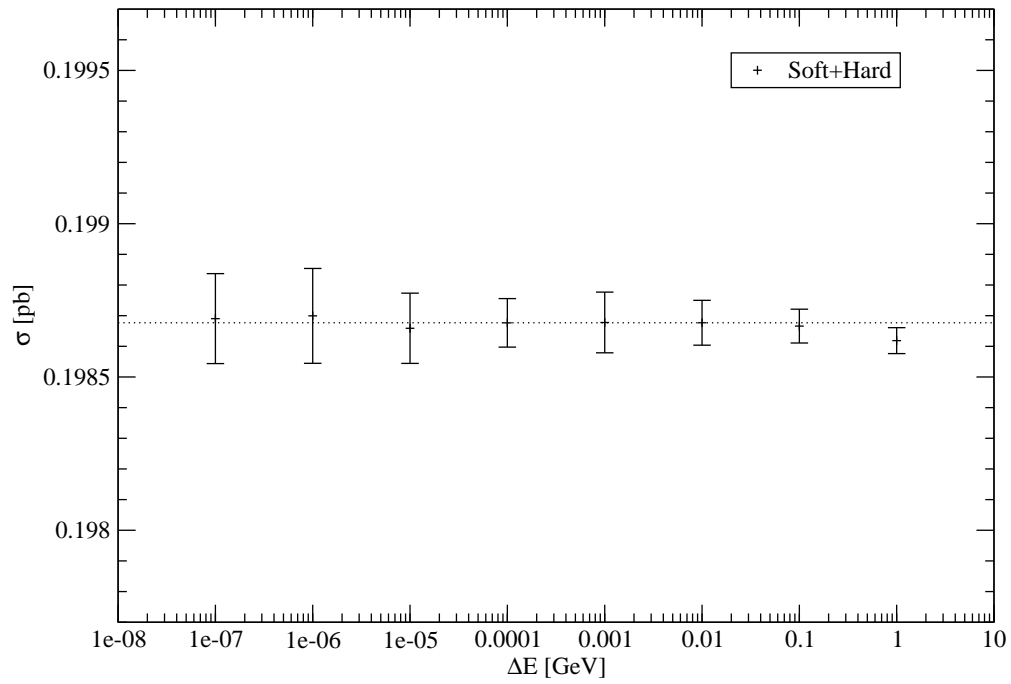
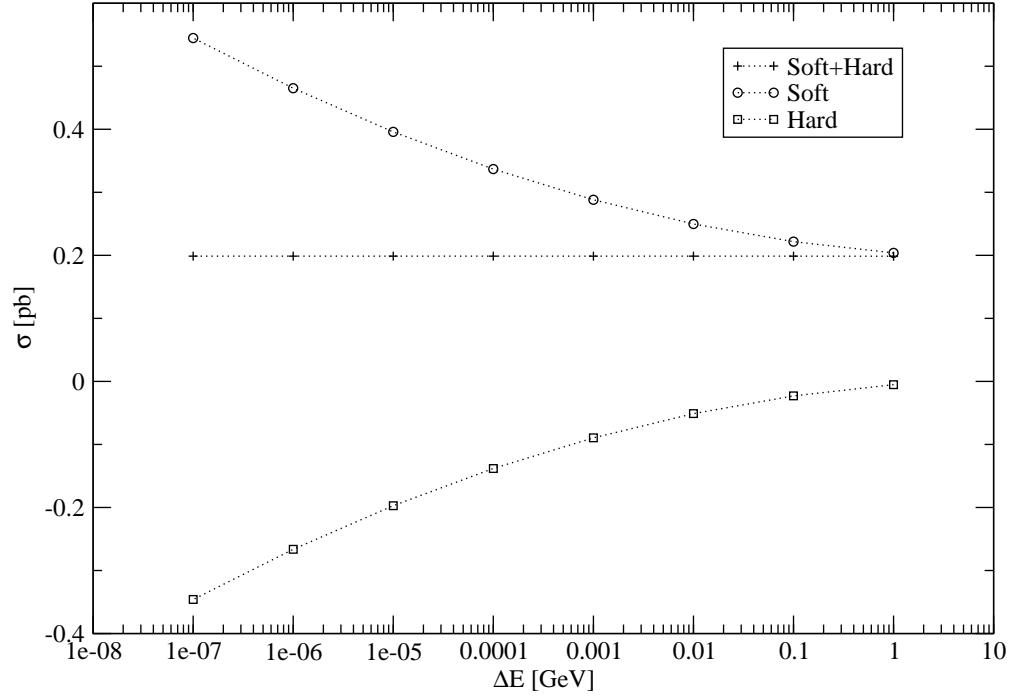


Figure 2: Upper panel: dependence of the $\mathcal{O}(\alpha)$ soft plus virtual and hard cross sections on the soft-hard separator ΔE . Lower panel: independence of the sum of $\mathcal{O}(\alpha)$ soft plus virtual and hard cross sections of the separator ΔE .

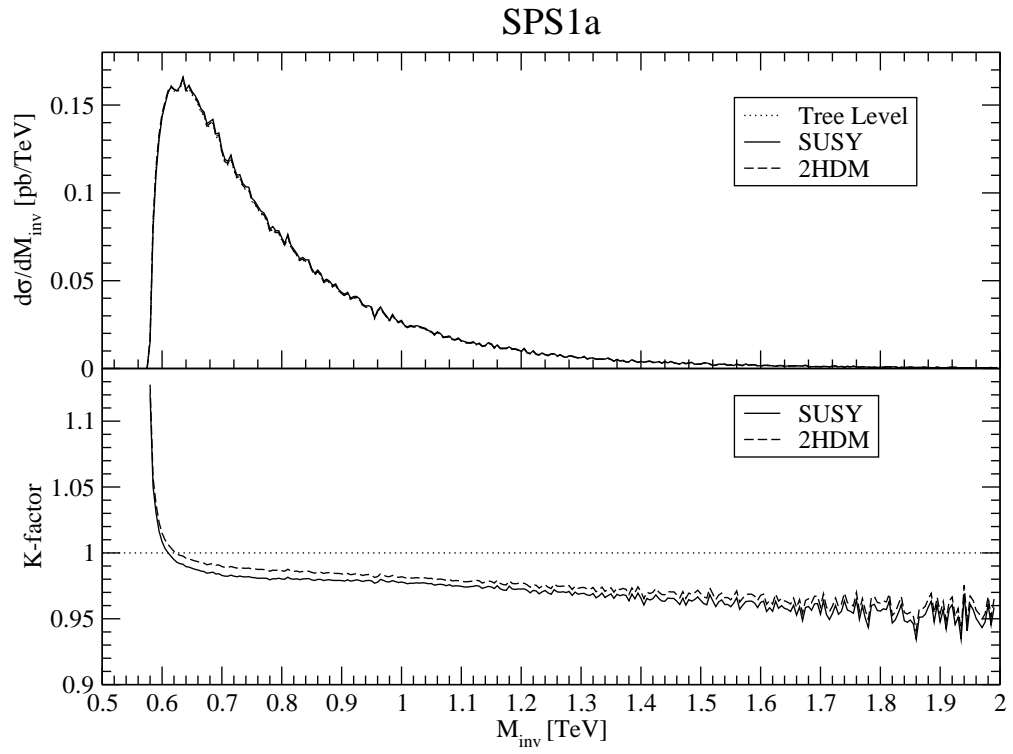
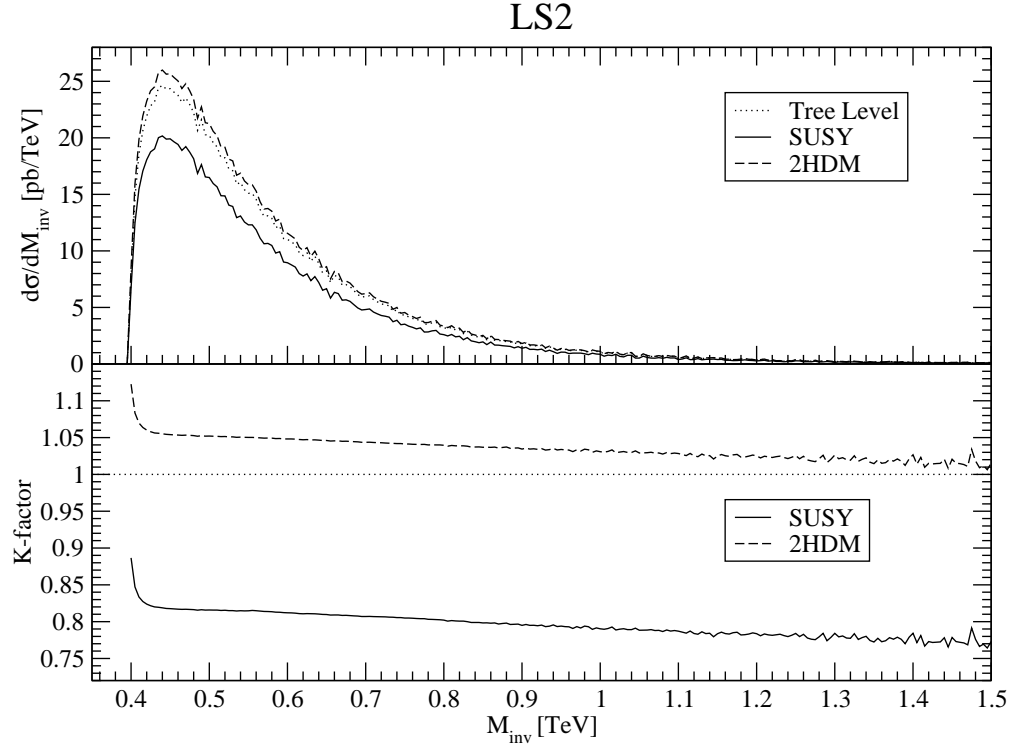


Figure 3: Differential distribution (upper panels) and partial K-factors (lower panels) in LS2 and SPS1a.

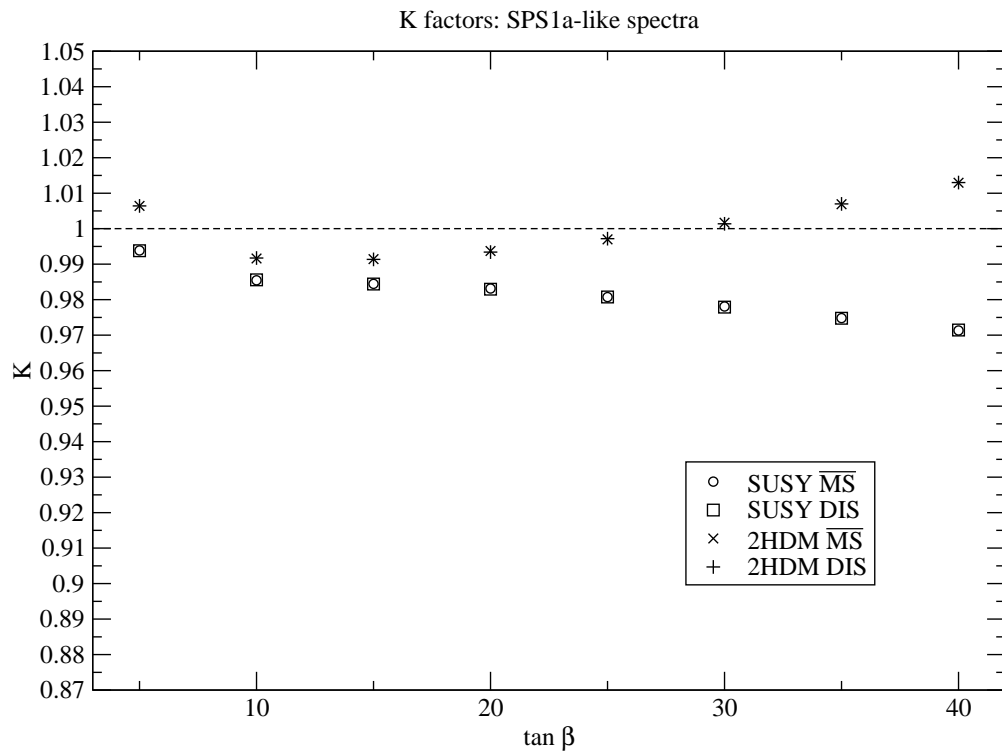
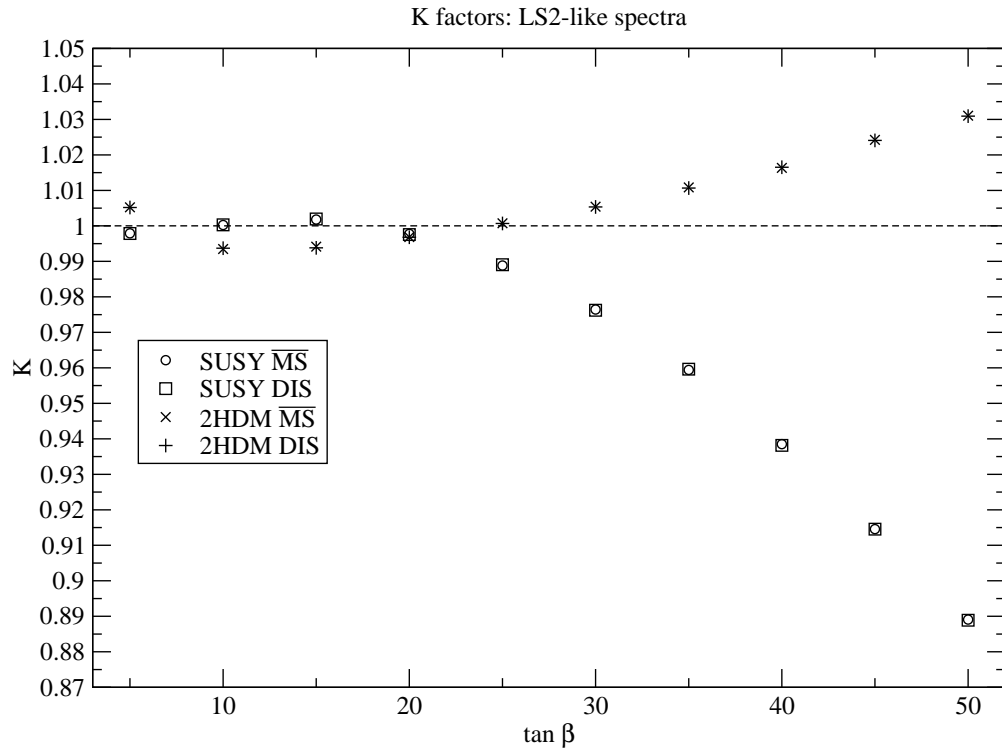


Figure 4: K-factor dependence on $\tan \beta$ for LS2- and SPS1a-like spectra.

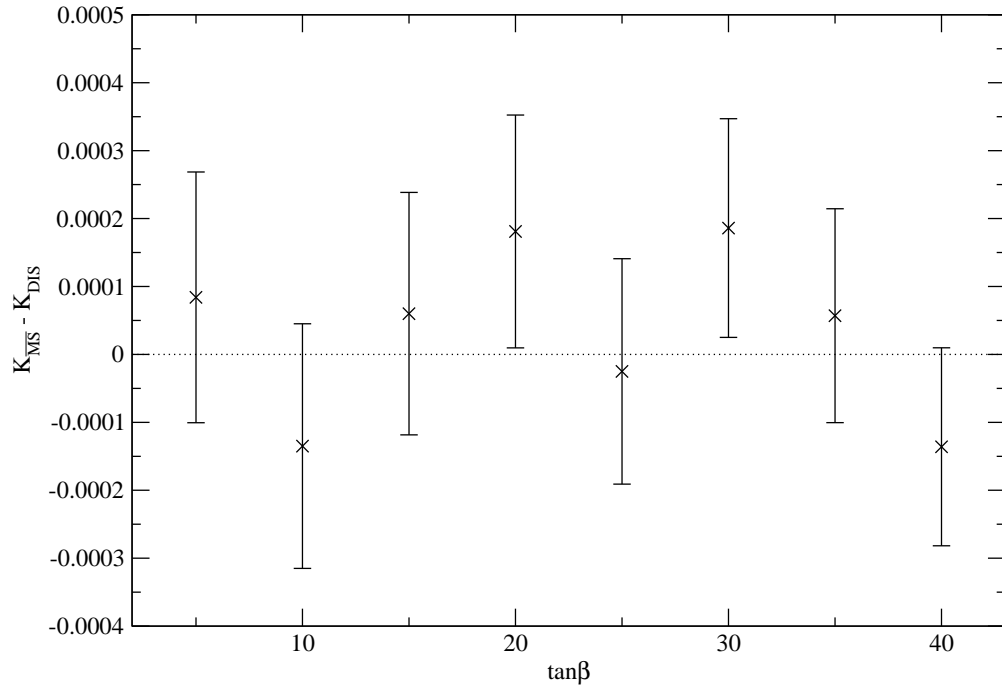


Figure 5: Factorization scheme dependence of the K-factor